Vibrational Structure of GDP and GTP Bound to RAS: An Isotope-Edited FTIR Study†

Hu Cheng, Sean Sukal, Hua Deng, Thomas S. Leyh,* and Robert Callender*

Department of Biochemistry, Albert Einstein College of Medicine, Bronx, New York 10461

Received September 7, 2000; Revised Manuscript Received January 9, 2001

ABSTRACT: A complete vibrational description of the bonding of a ligand to a protein requires the assignment of both symmetric and antisymmetric vibrational modes. The symmetric modes of isotopically enriched enzyme-bound ligands can be obtained by Raman difference spectroscopy, but until now, the antisymmetric modes, which require IR difference spectroscopy, have not been generally accessible. We have developed the methodology needed to perform IR difference spectroscopy, assign the antisymmetric modes, and accurately describe bonding. The method is used to assess the bonding changes that occur as Mg·GDP and Mg·GTP move from solution into the active site of RAS. Binding to RAS opens the nonbridging, O⋯P⋯O angle of the γ-phosphate of GTP by 2.7°, yet the angular freedom (dispersion of the O⋯P⋯O angle) of the γ-phosphate is comparable to that in solution. In contrast, the motion of the β-phosphate of GDP is highly restricted, suggesting that it positions the γ-phosphate for nucleophilic attack. The β,γ-bridging O−P bond of bound GTP is slightly weakened, being lengthened by 0.005 Å in the active site, corresponding to a bond order decrease of 0.012 valence unit (vu). The observed binding changes are consistent with a RAS-mediated hydrolysis mechanism that parallels that for solution hydrolysis.

The bond length resolution of vibrational spectroscopy, which can be as accurate as ∼0.001 Å, is on par with that of small molecule X-ray diffraction. However, the vibrational spectroscopy of proteins (and other large molecules) is difficult to interpret because spectral crowding limits the assignment of vibrational bands to specific structural elements. Isotope editing in combination with accurate difference spectroscopy has proven to be a successful method for assignments in Raman spectroscopy (*1*). In this approach, key atoms of a ligand bound to a protein (or any other biomacromolecule in principle) are isotopically labeled, causing shifts in the frequencies of modes whose motion involves these atoms. The difference spectra of the labeled and unlabeled ligand−protein complex contain only the spectra of the labeled atoms; the remainder of the spectrum is nulled out. The water background in the IR is typically much stronger than in Raman; consequently, there has been limited use of isotope editing schemes in IR spectroscopy (*2*−*6*). To obtain sufficient subtraction accuracy, time-resolved IR difference spectroscopy has sometimes been used. Here, light switches the sample between two states. It is relatively easy to achieve a high degree of subtraction precision because, in this approach, the sample cell is not physically changed. Hence, there is virtually no change in the optical path between the two states. This approach has been used, for example, in IR experiments aimed at the RAS protein, the subject of this paper, through the use of caged GTP compounds which can be rapidly photolyzed (*7*, *8*). However, time-resolved methods have limited applicability (to systems that can be switched by light), while the very accurate assessment of bonding and bonding changes that is possible using vibrational spectroscopy typically requires assignment of both the symmetric (obtained from the Raman spectrum) and antisymmetric (from the IR) vibrational modes. This paper describes the development of a general technique that permits isotope editing in static IR spectroscopy even when the water background is very strong. The method is used to assess the bonding changes associated with the binding of nucleotides, Mg·GDP and Mg·GTP, to c-H-p21-ras (RAS).

RAS is a cellular messenger whose importance in mammalian tumorigenesis has resulted in intensive studies of RAS function at the molecular, cellular, and organismic levels. RAS plays essential roles in regulating the cell cycle (*9*, *10*), apoptosis (*11*), mitogen-activated protein kinase pathways (*12*, *13*), and retroviral activation (*14*). Integration of RAS structural and functional studies has resulted in paradigms that are used widely to interpret the behavior of many of the highly conserved proteins that define the GTPase superfamily (*15*). This study focuses primarily on determing how the β,γ-bond of GTP is cleaved (Scheme 1) at the active site of RAS.

Scheme 1

$$GTP^{4-} + H_2O \leftrightarrow GDP^{3-} + HPO_4^{2-} + H^+$$

Toward this end, the complete vibrational structures of Mg·GDP and Mg·GTP in solution, and at the active site of RAS, were obtained and compared to assess the bonding changes

† This work was supported in part by grants from the Institute of General Medicine, National Institutes of Health (GM35183 to R.C. and GM54469 to T.S.L.), and the National Science Foundation (MCB-9727439 to R.C.).

* To whom correspondence should be addressed: Department of Biochemistry, Albert Einstein College of Medicine, Bronx, NY 10461. Phone: (718) 430-3024. Fax: (718) 430-8565. E-mail: call@aecom.yu.edu.

10.1021/bi0021131 CCC: $20.00
Published on Web 03/06/2001

that occur when these substrates bind to the enzyme. The observed structural changes clearly indicate that the bridging $O-P_\gamma$ bond of GTP (the cleaved bond) weakens as GTP moves from solution to the active site environment. The decreased $O-P_\gamma$ bond order suggests that RAS uses a classical catalytic strategy in which cleavage is accelerated over solution by decreasing the pK_a of the GDP leaving group.

MATERIALS AND METHODS

Oligonucleotides were supplied by the Albert Einstein College of Medicine Oligonucleotide Synthesis Facility. Restriction enzymes were purchased from New England Biolabs. Pfu polymerase was from Strategene, and the pET-23a(+) plasmid and BL21(DE3) *Escherichia coli* cells were from Novagen. PCl_5, nucleotides, and enzymes used for the syntheses were from Sigma Chemical Co. and were of the highest available grade. Buffers, solvents, and culture media were from Fisher Scientific or from Sigma Chemical Co. KCNO was from Acros Organics. PEI F-cellulose TLC plates were from EM Science. The ^{18}O-labeled water was from Isotec (96.2 at. % ^{18}O). Radionucleotides were from NEN Life Science Products. The Q Sepharose Fast Flow resin was from Pharmacia, and the P6 spin columns were from Bio-Rad.

Construction of the Ras Expression Vector. The DNA coding sequence for amino acids 1−166 of human RAS was amplified by oligonucleotide-directed PCR from a yeast expression plasmid containing the full-length sequence of the human gene, a generous gift from T. Michaeli. Oligonucleotides 5′-ATTCCATATGACCGAATACAAACTGG-3′ and 5′-GCGGATCCGTTAGTGCTGACGGATTTCAC-GAAC-3′ were designed to contain *Nde*I and *Bam*HI restriction sites at the 3′ and 5′ ends of the amplified product. The product was cloned into the pET-23a(+) overexpression plasmid. SDS−PAGE analysis of the overexpression in BL21(DE3) *E. coli* cells showed that the soluble cellular fraction that contained p21-ras was at least 10% of the total soluble protein.

Purification of Ras. The protein was purified according to standard published procedures (*16*, *17*). The protocol yielded approximately 10 mg/L of cell culture of >95% pure p21-ras as judged by SDS−PAGE. The protein was stored at −70 °C in the presence of 0.10 mM GDP.

Ras Activity Assay. A 52 μM p21-ras solution was made by diluting a concentrated enzyme stock with an appropriate buffer to achieve the following final buffer concentrations: 50 mM Tris (pH 7.5), 20 mM EDTA, 200 mM $(NH_4)_2SO_4$, and 10 mM DTT at 25 °C. After a 5 min incubation, the solution was loaded onto a P6 spin column equilibrated in 50 mM Tris (pH 7.5) and 10 mM DTT. GTP and the [γ-^{32}P]-GTP tracer (1.2 active site equivalents) was placed in the column's collection tube. The nucleotide free p21-ras was eluted directly into this mixture by centrifugation. RAS was nucleotide free for less than 1 min. $MgCl_2$ was added to a final concentration of 10 mM to begin the 80 min time course. Aliquots were removed at 10 min intervals and brought to 200 mM in EDTA to stop the reaction. Each point was spotted on PEI F-cellulose TLC plates and developed in 0.9 M LiCl buffer. The GTP and phosphate spots were quantitated on an AMBIS scanner. The time course was fit to a single exponential, and the calculated turnover number was 0.013 ± 0.005 min^{-1} at room temperature and 0.00029 min^{-1} at 4 °C.

[γ-$^{18}O_3$]GTP Synthesis. Fresh PCl_5 (458 μmol) was added to a 30-fold molar excess of rapidly stirred ^{18}O-labeled water in an oven-dried tube. The solution was neutralized with 10 M KOH. One equivalent (458 μmol) of sodium acetate was added from a 1 M stock. The solution was diluted 2-fold with water, and 7.5 molar equiv of KCNO was added from a 6 M freshly prepared stock solution. This reaction mixture was kept at 30 °C and pH 6.5 by addition of glacial acetic acid in 5 min intervals for 30 min. An additional 2 molar equiv of KCNO was added, and the temperature and pH monitoring continued for an additional 30 min. One mole fraction of ADP [458 μmol, 0.58 M Tris (pH 7.3), 116 mM $MgSO_4$ buffer] was then added, followed by 17 units (micromoles per minute) of carbamate kinase. The reaction mixture was incubated at 38 °C for 30 min to convert the ADP and carbamyl phosphate to [γ-$^{18}O_3$]ATP.

The nucleotide was diluted to a final concentration of 5.5 mM with 11 mM Tris (pH 7.5) and 11 mM $MgSO_4$ buffer, and 5 molar equiv of GDP was added. Two hundred units of nucleoside-5′-diphosphate kinase was added and the mixture incubated at 37 °C for 1 h. The nucleotide was purified after this time on a Q-Sepharose Fast Flow anion exchange column using a 10 mM to 1.2 M triethylamine bicarbonate (pH 7.6) linear gradient. The GTP eluted at 0.97 M triethylamine bicarbonate. Fractions containing [γ-$^{18}O_3$]-GTP were pooled and rerun under similar conditions to remove any traces of contaminating nucleotides. The GTP was then rotary evaporated to dryness and washed with methanol and water to remove the triethylamine. The nucleotide was dissolved in water, brought to pH 8.5 with 10 M KOH, and stored at −70 °C. The [γ-$^{18}O_3$]GTP was judged to be greater than 95% pure by TLC on PEI F-cellulose plates.

[β-$^{18}O_3$]GDP Synthesis. [γ-$^{18}O_3$]ATP was synthesized by the carbamate kinase reaction as described above. It was necessary to purify the [γ-$^{18}O_3$]ATP (Q-Sepharose Fast Flow 0 to 1.0 M KCl linear gradient) from this reaction mixture since the guanylate kinase used in the subsequent step lost activity. One hundred twenty micromoles of this [γ-$^{18}O_3$]-ATP, 9.6 mmol of GMP, 1 mmol of $MgCl_2$, and 0.1 mol of KCl were brought to pH 8.0 with Tris base in a total volume of 1 L. It was necessary to run this reaction at low concentrations of nucleotide since GMP had to be used at an 80-fold molar excess to achieve optimal product formation and was insoluble at higher concentrations. Guanylate kinase (2.5 units) was added to the mixture at room temperature every hour for 5 h. The incubation was continued overnight at room temperature. A parallel reaction run using trace radiolabeled [γ-^{32}P]ATP showed that 91% of the starting ATP was converted to product. The [β-$^{18}O_3$]GDP was purified as described for the GTP above. The GDP eluted off the column at a TEA bicarbonate concentration of 0.76 M. The nucleotide was dissolved in water, brought to pH 7.0 with 10 M KOH, and stored at −70 °C. The [β-$^{18}O_3$]-GDP was judged to be greater than 95% pure by TLC.

Electrospray Mass Spectrometry. Mass spectrometry was performed at the Hunter College Mass Spectrometry Facility (New York, NY). An Agilent Technologies (formerly Hewlett-Packard) HP1100 LC/MSD instrument was used to

collect the electrospray spectra in the negative mode. The mass spectral analysis of the [γ-$^{18}O_3$]GTP and [β-$^{18}O_3$]GDP shows 89.6 and 88.0% enrichment in ^{18}O, respectively.

Nucleotide Exchange. RAS complexed with (^{18}O)GDP-(GTP) was prepared in two stages. First, purified RAS was concentrated and washed with buffer I [200 mM Tris-HCl, 200 mM $(NH_4)_2SO_4$, 0.55 mM DTT, 0.5 mM NaN_3, and 0.6 mM EDTA (pH 7.5)] to remove excess GDP and Mg^{2+}. The protein was then incubated for 30 min at room temperature with a 10-fold molar excess of (^{18}O)GDP(GTP) in buffer I. After that, several approaches were taken according to different requirements of the various experiments.

To observe the phosphate IR bands of RAS·GTP, samples were exchanged into buffer II [20 mM Tris-HCl, 10 mM $MgCl_2$, and 0.5 mM NaN_3 (pH 7.5)] using a Centricon 10 concentrator. The final concentration was made as high as possible (2−6 mM) to obtain best signal-to-noise ratio in the IR spectra. The pH of the solution was adjusted with HCl or NaOH.

Spectroscopy. FTIR spectroscopy was performed on an IFS-66 Fourier transform spectrometer (Bruker Instruments Inc., Billerica, MA) and a Magna 760 Fourier transform spectrometer (Nicolet Instrument Corp.) using a MCT detector in each case. Both reference and sample solutions were simultaneously loaded into a dual-cell shuttle accessory. BaF_2 sandwich cells with 25 μm Teflon spacers were used. A two-position sample shuttle was used to alternate between the sample and reference buffer positions; this procedure substantially decreased the spectral contribution of residual water vapor after subtraction. Spectra were collected in the range of 400−4000 cm^{-1} with 2 cm^{-1} resolution. A Blackman−Harris three-term apodization and a Happ−Genzel apodization were applied, respectively. Opus 2.0 (Bruker Instruments, Inc.) and Omnic 4.0a (Nicolet Instruments, Corp.) were used for data collection and analysis. The solvent background spectrum was subtracted from each protein solution spectrum. As the sample and reference cells were assembled separately, their path lengths were not completely equal. To correct for this, a previously measured solution spectrum was multiplied by a correction factor determined by requiring a baseline that is flat between 1750 and 2000 cm^{-1}.

RESULTS

IR Difference Spectroscopy. Our studies involve the use of isotope-edited IR difference spectroscopy. Here specifically, the three oxygens of the terminal phosphate group of GDP or GTP bound to RAS are isotopically labeled with ^{18}O, the IR spectra of the enzyme-bound ^{16}O- and ^{18}O-labeled nucleotides are taken, and a difference spectrum is formed by suitable subtraction of the $^{16}O/^{18}O$ pair. Conceptually, this difference spectrum contains only bands from normal modes involving motions of nonbridging oxygens of the phosphate group, and all others have canceled out. There are, however, a number of experimental constraints that apply to this procedure if an accurate difference spectrum is to be obtained. First, water has a substantial IR absorbance. Its IR spectrum in the 500−2000 cm^{-1} region contains a strong peak near 1630 cm^{-1} and several overlapping bands centered at ~750 cm^{-1}. The water absorbance is lower (OD ~ 0.4 for a 25 μm path length) and, importantly, relatively flat between ~1000 and 1500 cm^{-1}. We found that this background spectrum can be well nulled within this frequency range. Fortunately, this spectral range is well suited for the study of phosphates. (It would be possible, however, to perform measurements in the water background-blocked regions using D_2O since the 1630 and 750 cm^{-1} water bands are quite sensitive to isotope and shift to approximately 1200 and 600 cm^{-1}, respectively.) Second, the IR spectra must contain sufficient signal to noise so that the small spectral differences in the two parent spectra are not lost in the noise of the difference spectrum. Our previous studies (*1*) on isotope-edited Raman difference spectroscopy suggest that, for small- to medium-sized proteins, a signal-to-noise ratio of ~1000/1 is sufficient to observe reasonably intense IR bands in the difference spectrum. Hence, for a parent spectrum having an OD of 1, the spectrometer should be able to measure a protein spectrum of better than 1 mOD unit, which is easily achievable with most modern IR spectrometers (our setups include advanced models of two popular brands). This signal-to-noise consideration, however, requires that the protein signal be comparable to the background water spectrum. For a protein like RAS, a concentration of several millimolar is required to achieve optical density at major protein peaks, like the amide II band at 1550 cm^{-1}, of a few tenths of an OD unit for the 25 μm path length used in this study.

To avoid systematic drift or mismatch in the spectral registry of the sample and reference parent spectra, we built a computer-controlled shuttle attached to the plate of the sample holder area which brings the sample cell and reference cell into the IR beam of the spectrometer. Thus, the spectrometer, particularly the cell holder area, was minimally perturbed during the experiment. Keeping a tight spectral registry is crucial, and minimal disturbance of the spectrometer system during the experiment is important. This issue is discussed quite fully in our previous studies on Raman difference spectroscopy (*1*). Last, it is necessary to null out residual water vapor bands from both parent spectra. In our case, the IR spectrometer was well purged with dry air to minimize water vapor in the IR path within the spectrometer. In our hands, these bands were typically a few mOD units in the parent spectra and could be nulled out to a very high degree, better than about 0.0001 OD unit, by subtracting their spectrum as measured in a separate run. On the other hand, it is very difficult to have two cells (reference and sample) optically identical. Invariably, one cell's path length is slightly different than the other. Hence, the difference spectrum formed by simply subtracting the reference spectrum from that of the sample contains residual background protein, water, and/or buffer spectral features that are incompletely subtracted. In this case, we apply a small correction factor to one of the parent spectra which is varied until the background peaks null.

Figures 1 and 2 illustrate these considerations on the RAS system. Figure 1a shows the spectrum of RAS·Mg·GDP and labeled RAS·Mg·[β-$^{18}O_3$]GDP in 25 μm cells. These two spectra, virtually superimposable (although a close examination near 1100 cm^{-1} suggests a small difference) as shown in Figure 1a, are the starting spectra of the subtraction process. Panel b of Figure 1 shows the same two spectra after the water/buffer spectrum, taken separately, has been subtracted. The relatively large protein peak near 1550 cm^{-1}

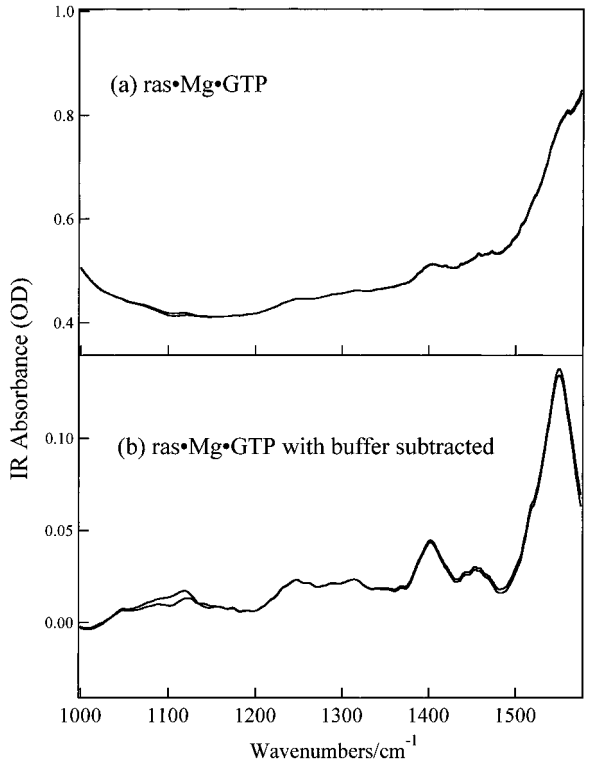

FIGURE 1: (a) IR spectra of 5 mM RAS·Mg·GTP and RAS·Mg·[γ-$^{18}O_3$]GTP in 20 mM Tris-HCl buffer at pH 7.5 and 4 °C. (b) Spectra from panel a with the spectrum of Tris buffer subtracted.

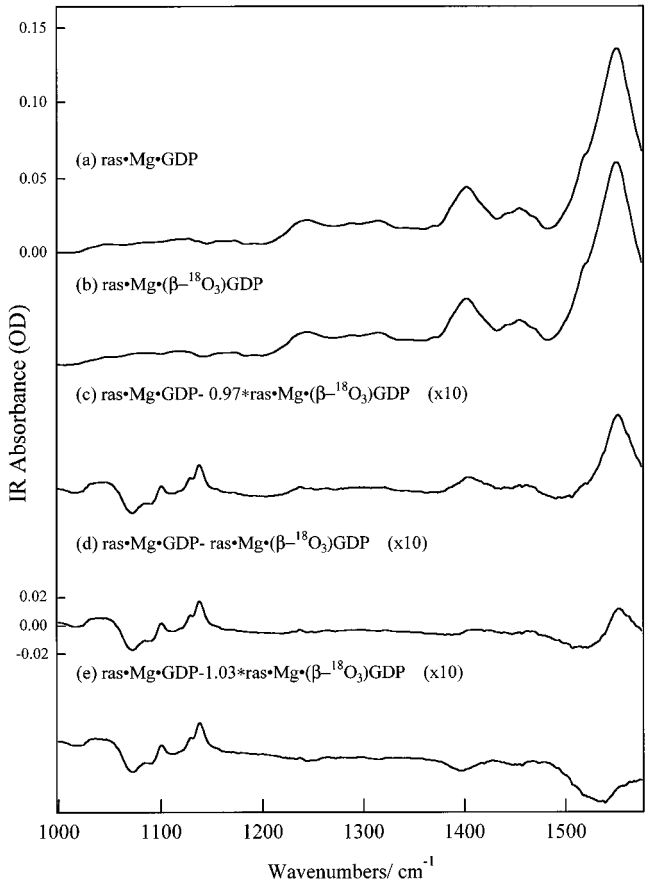

FIGURE 2: (a) IR spectrum of RAS·Mg·GDP, (b) IR spectrum of RAS·Mg·[γ-$^{18}O_3$]GDP, and (c) difference spectrum between RAS·Mg·GDP and RAS·Mg·[γ-$^{18}O_3$]GDP. The latter spectrum was multiplied by a factor of 0.97 before subtraction. The scale has been greatly amplified (see scale panel d) compared to that for spectra a and b. (d) Difference spectrum between RAS·Mg·GDP and RAS·Mg·[γ-$^{18}O_3$]GDP. The scale has been changed by a factor of ~10 compared to that for spectra a and b. (e) Difference spectrum between RAS·Mg·GDP and RAS·Mg·[γ-$^{18}O_3$]GDP. The latter spectrum was multiplied by a factor of 1.03 before subtraction. The scale has been greatly amplified (see scale panel d) compared to that for spectra a and b.

is the well-known amide II peak of proteins. Panels a and b of Figure 2 show, individually, the analogous two spectra given in Figure 1b except now for the GDP system. Panels c−e show the result of subtracting these two parent spectra, scaled by a factor of 10. Because of the different cell path lengths, a small scaling factor between the two parent spectra is adjusted until the protein peaks, which are easily identified and are not affected by substitution of ^{18}O on the substrate phosphate, are well nulled. Note that the amide II peak does not entirely subtract but yields a small "derivative"-like signal in the difference spectrum of panel d. This indicates a small amount of misregistry in the frequency calibration of the two parent spectra. It is probable that the misregistry results from the substantial water background slope that begins near 1500 cm^{-1} (see Figure 1a). In such a series of difference spectra, it is most important to observe that the modes assigned to labeled phosphate groups (here, from 1050 to 1150 cm^{-1}) remain relatively constant as the background protein peaks range through an under- to oversubtracted situation.

Figure 3a shows the IR difference spectrum formed by subtracting the solution spectrum of Mg·[β-$^{18}O_3$]GDP from that of Mg·[β-$^{16}O_3$]GDP; panel b shows the analogous difference spectrum for GDP bound to RAS (this is the same as Figure 2d except over a narrow spectral range). A symmetric PO_3^{2-} moiety, as is reasonably well approximated for the terminal phosphate of GDP and GTP in solution, has three P···O stretch normal modes, a doubly degenerate antisymmetric stretch, ν_a, and one symmetric stretch, ν_s (see ref *18*). The antisymmetric stretch lies in the 1000−1200 cm^{-1} region and is strongly allowed in the IR. Therefore, the positive peak found in the solution difference spectrum at 1143 cm^{-1} arises from the antisymmetric stretch for RAS·[β-$^{16}O_3$]GDP, while the negative-going feature at 1086 cm^{-1} is ν_a for RAS·[β-$^{18}O_3$]GDP. The antisymmetric bands for Mg·GDP in solution have been previously measured (*19*) and lie at 1123 and 1089 cm^{-1} for [β-$^{16}O_3$]GDP and [β-$^{18}O_3$]-GDP, respectively. The fact that the peaks in the difference spectrum do not correspond to those found in the parent spectra has to do with the fact that the antisymmetric bands are broad relative to the 34 cm^{-1} shift that arises from the isotope labeling. In this case (*20*), the apparent band positions in the difference spectra are shifted, and the difference in frequency between the positive and negative couplet is greater than the isotope shift. The positions and bandwidths (full width at half-maximum, Γ) of the P···O stretches for Mg·GDP in water and bound to RAS have been summarized in Table 1. The symmetric stretch parameters have been taken from refs *19* and *21*. A previous time-resolved IR study, which employed caged GTP compounds of individually labeled ^{18}O P···O bonds and kinetic difference spectroscopic techniques, placed the IR modes of GDP bound to RAS at 1100 and 1236 cm^{-1} (*7*). We do not know the reason for the discrepancy between the two studies, although (*1*) the nature of individually labeling the oxygens distorts the symmetry of the β-phosphoryl group, making a strict comparison

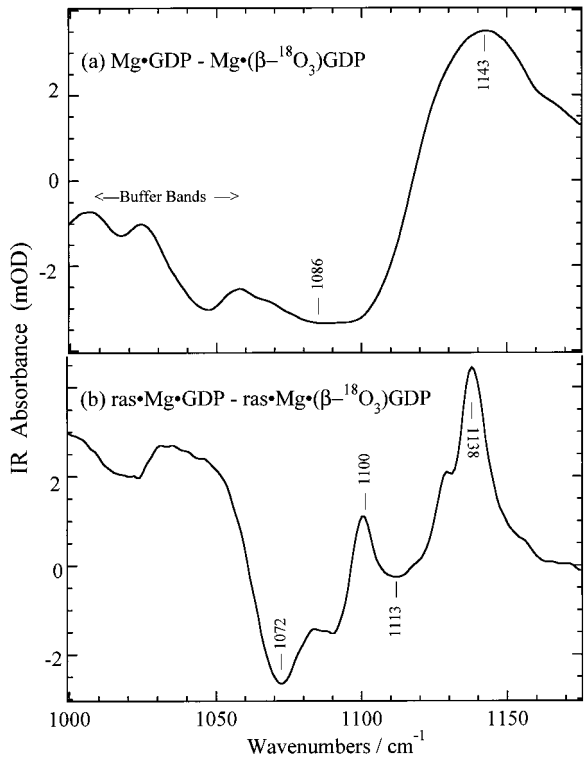

FIGURE 3: IR difference spectrum of the Mg·GDP complex minus that of the Mg·[β-$^{18}O_3$]GDP complex in (a) aqueous solution and (b) RAS at pH 7.5 and 4 °C.

Table 1: Frequencies (in cm^{-1}) of the Symmetric, ν_s, Antisymmetric, ν_a, and "Fundamental", ν, Stretch Modes of the Nonbonded P···O Stretch Modes of the β-Phosphate of GDP in Water and When Bound to RAS, the Bandwidth (half-width at half-maximum in cm^{-1}) of the Antisymmetric Mode, $\Gamma_{\nu a}$, Bond Orders, S (in vu), and Bond Lengths, R (in Å), of Nonbridging and Bridging Bonds, and the Approximate Root Mean Square of the Variation in the Angle (deg) of the Nonbridging O···P···O Bonds, $\Delta\theta$, Due to the Heterogeneous Broadening

	Mg·[β-$^{16}O_3$]GDP in water	RAS·Mg·[β-$^{16}O_3$]GDP
ν_s	942	915
ν_a	1123[a]	1138[a]
		1100[a]
ν	1066	1056
$S_{(\beta-\text{nonbridging P···O})}$	1.327	1.316
$S_{(\text{bridging O–P})}$	1.020	1.052
$R_{(\text{bridging O–P})}$	1.613	1.601
Γ_{ν_a}	62	~10
$\Delta\theta$ of O···P···O bonds	4.0° (±0.6°)	<0.7°

[a] The doubly degenerate antisymmetric stretch, ν_a, has been lifted for RAS-bound GDP.

difficult and (*2*), assignments of GDP bands rest on double difference spectra that are somewhat difficult to interpret (*8*). On the other hand, our results are in good agreement with a second study using caged compounds (*8*).

As ligands bind to proteins, their vibrational motion becomes restricted by interaction with the binding site. This restriction narrows the bands within the spectrum (particularly water). Comparison of panels a and b of Figure 3 demonstrates this narrowing effect on the β-phosphoryl group of GDP. The bandwidths in the protein difference spectrum are small enough that the apparent band positions lie at their true positions.

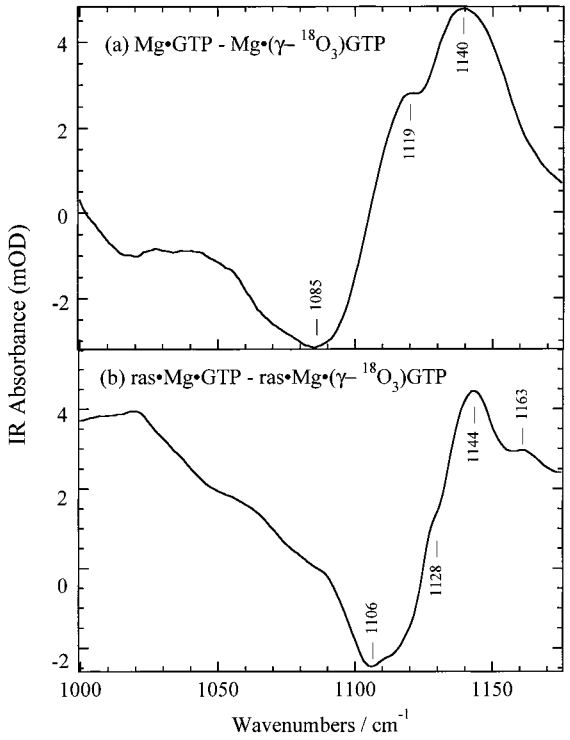

FIGURE 4: IR difference spectrum in aqueous solution at pH 7.5 and 4 °C: (a) Mg·GTP minus Mg·[γ-$^{18}O_3$]GTP and (b) RAS·Mg·GTP minus RAS·Mg·[γ-$^{18}O_3$]GTP.

It is clear from the observation of two positive/negative couplets in the difference spectrum, which are separated by the expected $^{16}O-^{18}O$ isotope shift, that the degeneracy of the antisymmetric modes is lifted by ligand binding interactions, and that the two frequencies lie at 1138 and 1100 cm^{-1}. This means that the approximate C_{3v} symmetry of the PO_3^{2-} moiety has been broken as would happen if, for example, one of the oxygens interacted through hydrogen bonding interactions with protein moieties that were stronger than the interactions with the other two. Such symmetry breaking has been observed for vanadate bound to the ATP binding site of myosin (*22*).

Figure 4a shows the IR difference spectrum formed by subtracting the solution spectrum of Mg·[γ-$^{18}O_3$]GTP from Mg·[γ-$^{16}O_3$]GTP, while panel b shows the phosphate difference spectrum for GTP bound to RAS. Although RAS catalyzes the hydrolysis of GTP to GDP, the half-time of the reaction on the enzyme is about 34 h at 4 °C, which is substantially longer than the time for these measurements (typically a few hours). In contrast to the GDP spectra, the solution and RAS-bound GTP difference spectra are similar. The C_{3v} symmetry of the γ-PO_3^{2-} moiety does *not* appear to be broken when GTP binds to RAS, and the degenerate ν_a bandwidth of both spectra is broad, causing the true peak positions to lie at somewhat different positions from the positive/negative positions of the couplet in the difference spectra. Figure 4 lists the positions of the couplet observed in the difference spectrum, while Table 2 lists the actual positions (*19*). The positions in Table 2 for ν_a in RAS·[γ-$^{16}O_3$]GTP come from calculating the difference of the shift in the average of the minimum and maximum position in the water and RAS difference spectra and adding this to the known water position. This procedure has been shown to give good values for shifts (*20*) even if the bandwidths are

Table 2: Frequencies (in cm^{-1}) of the Symmetric, ν_s, Antisymmetric, ν_a, and "Fundamental", ν, Stretch Modes of the Nonbonded P···O Stretch Modes of the γ-Phosphate of GTP in Water and When Bound to RAS, the Bandwidth (half-width at half-maximum in cm^{-1}) of the Antisymmetric Mode, $\Gamma_{\nu a}$, the Bond Orders, S (in vu), and Bond Lengths, R (in Å), of Nonbridging and Bridging Bonds, the Approximate Root Mean Square of the Variation in the Angle of the Nonbridging O···P···O Bonds, $\Delta\theta$, Due to the Heterogeneous Broadening, and the Angle, θ, of the Nonbridging O···P···O Bonds

	Mg·[γ-$^{16}O_3$]GTP in water	RAS·Mg·[γ-$^{16}O_3$]GTP
ν_s	926	916
ν_a	1128	1138
ν	1065	1069
$S_{(\text{nonbridging P···O})}$	1.326	1.330
$S_{(\text{bridging O−P})}$	1.023	1.011
$R_{(\text{bridging O−P})}$	1.611	1.616
Γ_{ν_a}	42	26
$\Delta\theta$ of O···P···O bonds	2.7° (±0.5°)	~1.8°
θ of O···P···O bonds	~115°	115° ± 2.1°

affected by binding. The position for ν_a measured here is in good agreement with the previous IR studies using caged GTP compounds and singly labeled P···O bonds which place an IR active mode at 1143 cm^{-1} for one of the γ-phosphate P···O stretch modes of bound GTP (*7*) and at 1142 cm^{-1} (*8*). The latter IR study, however, assigned a band at 1158 cm^{-1} to a second antisymmetric mode suggested to arise from lifting the C_{3v} symmetry of the γ-PO_3^{2-} moiety for bound GTP. Their observation may correspond to the weak mode located at about 1163 cm^{-1} in Figure 4b in our study. We believe that this band is not a second antisymmetric mode for the following reasons. (1) The band is quite small in intensity (the two bands should have quite similar intensities). (2) It appears as a weak shoulder in the GTP solution data (Figure 4a). (3) The bandwidth of the 1144 cm^{-1} mode is quite broad, indicating weak interactions at the active site with the γ-PO_3^{2-} moiety. (4) The band also seems to appear in the GDP data of Figure 3. It may correspond to one of the O−P−O bending modes. The bandwidth of the antisymmetric mode of the γ-phosphate for Mg·GTP in water comes from ref *19*. The bandwidth of the GTP-bound mode was estimated by fitting the difference spectrum to trial Gaussian functions of varying half-widths. The positions for ν_s in RAS·[γ-$^{16}O_3$]GTP have been previously measured (*19*, *21*).

Vibrational Data Analysis. Accurate, empirically derived relationships between vibrational frequency and bond length (or bond order) have been developed for phosphate P···O and P−O bonds (*18*, *21*). The bond order convention used in this analysis imposes the constraint that the sum of the spectroscopic bond strengths for atoms is fixed to atomic valence, which for phosphates is 5.0. Such a bond valence paradigm has been shown to yield very accurate bond length refinements in crystallographic studies when coupled to the network theory of Brown and co-workers (*23*−*25*). The bond orders (bond strengths) are given in terms of valence units (vu).[1] The second leg of the analysis rests on relating vibrational frequencies to bond lengths. This relationship has been empirically determined by relating the vibrational frequencies to the bond lengths observed in small molecule crystallography, and the procedure has strong theoretical underpinnings (*18*). The equations that define these relationships for phosphates are (*18*)

$$S_{PO} = (R_{PO}/1.620)^{-4.29} \quad (1)$$

$$S_{PO} = [0.175 \ln(224500/\upsilon)]^{-4.29} \quad (2)$$

where S_{PO} is the bond order of the PO bond, R_{PO} is the length of the PO bond, and υ is the geometric average frequency of the phosphate stretch or "fundamental frequency" for dianionic phosphate esters that preserve the C_{3v} symmetry of the PO_3^{2-} moiety, as given by

$$\upsilon = [(\upsilon_s^2 + 2\upsilon_a^2)/3]^{1/2} \quad (3)$$

In this case, the average bond order and bond length of the nonbridging P···O bonds are the same as those of each individual P···O bond. When the PO_3^{2-} symmetry is not retained, as is the case for the β-phosphate group of GDP bound to RAS, the fundamental frequency is defined by eq 4

$$\upsilon = [(\upsilon_1^2 + \upsilon_2^2 + \upsilon_3^2)/3]^{1/2} \quad (4)$$

and, when used in eq 2, yields an average, nonbridging P···O bond order. An average nonbridging P···O bond length can then be calculated from eq 1. By setting eqs 1 and 2 equal to each other, we derived a direct function between bond length and frequency. In this way, bond lengths and bond orders can be determined if the stretch frequencies are known. The error in the absolute value of the bond lengths obtained from this method has been estimated to be ±0.004 Å by comparing spectroscopically determined bond lengths to small molecule diffraction studies and from theory (*18*). This suggests an absolute error of ±0.012 vu in determining bond orders using eq 1. A large part of this error has to do with mode coupling between P···O stretches and other modes which affects the character of the stretch mode to some extent and which varies among various phosphate compounds. An accuracy of ±0.004 Å relates to an error of ±13 cm^{-1} using eqs 1 and 2 to relate frequency to bond length. The precision of the measurement of vibrational frequencies is much better than this, about ±2 cm^{-1}, and the issue of mode−mode coupling is not as important for the same molecule in different environments (i.e., the coupling parameters remain essentially constant). Hence, the changes of these parameters, as in the case of a specific molecule changing from one environment to another like the binding of nucleotide to RAS, are more accurately determined. It is unclear what the accuracy is since there are no experimental benchmarks. However, an accuracy of better than ±0.001 Å is possible using the ultimate accuracy provided by the precision in the measurement of frequency. Tables 1 and 2 list the bond lengths and bond orders of the nonbridging P···O bonds and the bridging O−P bond using eqs 1 and 2 while holding the sum of the bond order about the phosphorus atom to 5 (*26*).

The positions of the symmetric and antisymmetric modes of phosphate depend on the angle, θ, between the nonbridging O···P···O bonds of the PO_3^{2-} moiety and the ratio of the stretch force constant for the P···O bond to the P···O/P···O stretch/stretch off-diagonal force constant. Using ab initio calculations (at the HF/3-21g* level), we have esti-

[1] Abbreviation: vu, valence unit (a measure of bond order based on atomic valence).

mated (*21*) that $\theta \sim 115°$ for the terminal PO_3^{2-} group of a triphosphate, agreeing well with the average angle of ATP molecules found in the Cambridge Structural Database, which is about 113.5° (an angle of 120° means a planar PO_3^{2-} moiety as would be found, for example, in metaphosphate; *21*). The *change* in the angle of the PO_3^{2-} moiety as GTP binds to RAS can be estimated from changes in the two frequencies. At the time of our previous study, the position of the antisymmetric mode for the γ-phosphate of GTP bound to RAS was not determined. Given that $\upsilon_s = 916$ cm^{-1} and $\upsilon_a = 1138$ cm^{-1} for RAS·Mg·[γ-$^{16}O_3$]GTP (Table 2), it is calculated that the θ of O···P···O bonds widens by about +2.1° (i.e., becoming substantially more planar) when the nucleotide binds (*21*).

The widths of antisymmetric stretch modes of dianionic monoesters in solution are quite broad (42 cm^{-1} for GTP in water), while those of symmetric stretch modes are relatively narrow (<10 cm^{-1} for GTP). This is due to varying values of θ arising from the heterogeneous structure of the nucleotide and concomitant heterogeneous broadening of the antisymmetric mode (*18*). The symmetric mode frequency is not sensitive to varying values of θ for the particular structure of GTP. From the width of the antisymmetric stretch, we estimated previously (*18*, *21*) that the angle ($\Delta\theta$) of the O···P···O group of the PO_3^{2-} moiety ranges over about 2.7° (±0.5°) for GTP in aqueous solution. It is clear (Figure 4b) that the antisymmetric bandwidth is smaller for GTP bound to RAS than for GTP in water. We estimate that the width of the stretch mode is reduced to 26 cm^{-1}, and this reduces the excursion of the O···P···O angle to 1.8°. Similar calculations yield the variation in θ values for GDP in water and when bound to RAS from the data of Figure 3 and are listed in Table 1.

DISCUSSION

This study examines the structure of the terminal phosphate group of GDP and GTP bound to RAS using isotope-edited IR difference spectroscopy. Vibrational spectroscopy is a particularly valuable probe of the ground-state distortions that an enzyme imposes on the bound substrate to potentiate chemistry. These distortions result in bond length changes on the order of 0.1−0.001 Å, which is within the accuracy of the method. Our main interest here is how RAS binds GDP and GTP nucleotides and how it brings about hydrolysis of the γ-phosphate of bound GTP. We have previously studied this issue using Raman difference spectroscopy (*21*). The symmetric stretch modes of phosphate groups are Raman active, while the antisymmetric stretches are IR active. To employ the empirical relationships between structure and vibrational frequencies (see Results), both symmetric and antisymmetric stretches must be known. Hence, an IR study provides the complete measurement of the vibrational structure of GDP and GTP bound to RAS, permitting a determination of the changes in bond lengths and bond orders in key bonds that are brought about by binding. Moreover, the bandwidths of these modes, especially the antisymmetric modes of the PO_3^{2-} moiety, are valuable measures of conformation flexibility that is available to the phosphate group. Ultimately, this highly accurate structural picture of the bound nucleotide can be related to mechanism.

The measurement of the antisymmetric modes of RAS-bound GDP or GTP has been approached in two previous studies using time-resolved FTIR studies of "caged" GTP analogues (*7*, *8*). In one study (*7*), individual P···O bonds were labeled with ^{18}O to make assignments rather than all three nonbridging phosphate bonds as used here. This results in a different approach to making the band assignments. Our results of bound GTP are in reasonable agreement with the results of that study but differ with regard to bound GDP. The results presented here are in better agreement with the second study, which used a labeling scheme for band assignments similar to that used here, except with regard to the breaking of the degeneracy of the bound γ-phosphate group of RAS·GTP (we do not see evidence for degeneracy breaking). It is unclear to us if the use of caged compounds, which could alter protein conformation and structure, might give rise to signals in the time-resolved difference spectra.

In agreement with previous results (*7*, *8*, *21*), the terminal phosphate group of GDP is clearly highly immobilized when bound to RAS. This is seen most cogently in the >42 cm^{-1} collapse in the bandwidth of the β-phosphate antisymmetric mode that occurs as GDP moves from solution into the active site. The large solution bandwidth is a result, primarily, of the conformation flexibility of the PO_3^{2-} group in water with regard to the O···P···O angle. The antisymmetric mode stretch frequency is a sensitive function of this angle (*18*), and as the phosphate group accesses various conformations with regard to this coordinate, each conformation will result in a somewhat different antisymmetric P···O stretch frequency that gives rise to the heterogeneously broadened bandwidth of this mode. The estimated angle variation of the terminal phosphate group of GDP in the nonrigid, aqueous environment, based on the measure bandwidth, is about ±2° from equilibrium for a total of variation of 4°. This estimation is quite consistent with calculations on a model phosphate (methyl phosphate) using ab initio methods (b3lyp/6-31g* basis set; *21*). The calculations suggest that a change in the O···P···O angle from its equilibrium value by 2° costs only 0.4 kcal/mol. Thus, the variation of ±2° from equilibrium observed in solution is easily driven by thermal motion ($RT = 0.6$ kcal/mol). On the other hand, the O···P···O angle of the terminal phosphate for GDP bound to RAS is restricted to less than 0.7°.

In addition to the restricted angular motion of the β-phosphate, the interactions between the PO_3^{2-} group and the binding pocket of RAS break the approximate C_{3v} symmetry of the phosphate group. Two strong antisymmetric bands are observed in the IR. Using an ab initio quantum mechanical approach, we previously considered how various interactions between GDP and RAS could account for the observed vibrational phosphate stretch frequencies (*21*). It was found that the binding pocket Mg^{2+} cation would have a large effect on the frequencies of the β-phosphate, reducing the antisymmetric stretch by an average of 30 cm^{-1} from that found in solution (and also reducing the symmetric stretch by 34 cm^{-1}), which is in accord with the experimental observations. It was also found that, because the cation is closer to one of the P···O bonds relative to the other two (the geometry was taken from the crystallographic studies of the RAS·GDP complex; *27*, *28*), the degeneracy of the β-PO_3^{2-} group is lifted. Two antisymmetric-like modes were calculated, one shifted by −6 cm^{-1} and the other shifted by −54 cm^{-1} from the solution frequency. This is in semiquantitative agreement with the observed results (Table 1). Shifts

of this magnitude result from significant polarization of the nonbridging P⋯O bonds and are are indicative of quite strong ionic interactions between the phosphate moiety and the protein. These calculations show what is clear from the experimental results, i.e., that the binding pocket is quite antisymmetric with regard to the β-phosphate group of bound GDP. In summary, the β-phosphate group of RAS-bound GDP is tightly bound and relatively rigid.

On the basis of the frequency changes of the GTP terminal P⋯O stretch modes upon binding to RAS (Table 2), it can be calculated (see Results) that the average terminal P⋯O bond order is increased by 0.004 vu and that the average O⋯P⋯O angle is increased by ~2.1°. From this, the bond length of the terminal P−O bridging bond increases by at least 0.005 Å upon binding (Table 2). This is a rather small change but is, however, larger than experimental error (see Results). Our results also show that the bandwidth of the antisymmetric P⋯O stretch of GTP bound to RAS is still quite broad (26 cm^{-1}; Table 2). This line width corresponds to a dispersion in the O⋯P⋯O angle of about 1.8°, which is comparable to what is seen for Mg^{2+}•GTP in solution (i.e., 2.7°; Table 2). Thus, in contrast to the β-phosphate group of GDP, the active site has preserved the conformational flexibility of the γ-phosphate group of GTP bond angles close to that seen in solution, yet it causes the γ-PO_3^{2-} group to become substantially (2.1°) more planar. This enzyme-driven lengthening of the terminal bridging P−O bond and the opening of the O⋯P⋯O bond angle represents a structural destabilization of the γ-PO_3^{2-} group toward a more planar, or transition-state-like, structure. It is important to realize, however, that the energy cost of such changes is on the order of <1 kcal/mol since, as indicated above, ab initio calculations yield energies of this size on model phosphate systems for destabilization of the P−O bridging bond or O⋯P⋯O angle changes that are observed. Such destabilization energy in the ground state is very small compared to the solution-phase activation energy for GTP hydrolysis, ~25 kcal/mol (*29*, *30*).

The current studies provide an intimate view of the bonding changes that occur when Mg^{2+}•GTP binds to RAS and suggest that substrate begins to acquire transition-state-like features in the enzyme-bound ground state: the γ-PO_3^{2-} group approaches a more planar geometry expected in the transition state, and the bridging P−O bond is (slightly) weakened. In the solution chemistry of phosphoryl transfer of dianionic phosphate monoesters, it has been shown by classical analyses of Bronsted plots for hydrolysis versus changes in the pK_a of the RO^- leaving group that the structure of the transition state is primarily dissociative, i.e., RO^-⋯⋯PO_3^{2-}⋯⋯:NU, with :NU being the attacking nucleophile (*29*−*31*). Stabilization of this type of transition state suggests that ground-state effects on the electronic makeup of the molecule would be small since the ground state is so unlike this transition state in structure. However, stabilization of the RO^- leaving group, as observed in the present studies of bound GDP in RAS, is consistent with solution chemsitry and would leave a small signature in the ground state by weakening the bridging P−O bond of GDP−PO_3^{2-} as is observed. To make these qualitative considerations more quantitative, we have recently performed a series of measurements on RO−PO_3^{2-} molecules in water with varying leaving group (RO^-) stabilities (unpublished data). A very strong correlation exists between changes in bond order and phosphoryl transfer rates; a change in rate constant of a factor of 10 at 39 °C corresponds to a lengthening of the O−P bridging bond of 0.0023 Å over a very wide range, more than 10 decades, in rates. When this correlation is applied to RAS•GTP (which is not strictly valid since it has been developed for alcoholic leaving groups), the observed 0.012 vu decrease in the GTP $P_\beta O-P_\gamma$ bond order (Table 2) predicts a hydrolysis rate increased 140-fold over that in solution, which is ~10-fold less than what is observed in RAS (*32*). This is certainly in good semiquantitative agreement, especially considering the small changes that are observed. The correlation implies that the observed bonding changes lie on the reaction coordinate appropriate for a dissociative mechanism. It demonstrates that the magnitudes of the observed changes found in the solution chemistry are comparable to what is expected in the substrate ground state of a phosphate monoester dianion hydrolysis reaction in a classical dissociative reaction mechanism where the rate acceleration is on the order of what is provided by RAS.

REFERENCES

1. Callender, R., and Deng, H. (1994) *Annu. Rev. Biophys. Biomol. Struct. 23*, 215−245.
2. Baenziger, J. E., Miller, K. W., and Rothschild, K. J. (1992) *Biophys. J. 61*, 983−992.
3. Slaich, P. K., Primrose, W. U., Robinson, D., Drabble, K., Wharton, C. W., White, A. J., and Robert, G. C. K. (1992) *Biochem. J. 288*, 167−173.
4. Tonge, P. J., Pusztai, M., White, A. J., Wharton, C. W., and Carey, P. R. (1991) *Biochemistry 30*, 4790−4795.
5. Tonge, P. J., and Carey, P. R. (1993) in *Biomolecular Spectroscopy* (Clarke, R. J. H., and Hester, R. E., Eds.) pp 129−161, John Wiley and Sons Ltd., New York.
6. White, A. J., Drabble, K., Ward, S., and Wharton, C. W. (1992) *Biochem. J. 287*, 317−323.
7. Cepus, V., Goody, R. S., and Gerwert, K. (1998) *Biochemistry 37*, 10263−10271.
8. Du, X., Frei, H., and Kim, S.-H. (2000) *J. Biol. Chem. 275*, 8492−8500.
9. Peepers, D. S., Upton, T. M., Ladha, M. H., Neuman, E., Zalvide, J., Bernards, R., DeCaprio, J. A., and Ewen, M. E. (1997) *Nature 386*, 177−181.
10. Leone, G., DeGregori, J., Sears, R., Jakoi, L., and Nevinds, J. R. (1997) *Nature 387*, 422−426.
11. Cardone, M. H., Roy, N., Stennicke, H. R., Salvesen, G. S., and Franke, T. F. (1999) *Science 282*, 1318−1321.
12. Luttrell, L. M., Ferguson, S. S., Daaka, Y., Miller, W. E., Maudsley, S., Della Rocca, G. J., Lin, F., Kawakatsu, H., Owada, K., Luttrell, D. K., Caron, M. G., and Lefkowitz, R. J. (1999) *Science 283*, 655−661.
13. Marais, R., Light, Y., Mason, C., Paterson, H., Olsen, M. F., and Marshall, C. J. (1998) *Science 280*, 109−112.
14. Coffey, M. C., Strong, J. E., Forsyth, P. A., and Lee, P. W. (1998) *Science 282*, 1332−1334.
15. Scheffzek, K., Ahmadian, M. R., and Wittinghofer, A. (1998) *Trends Biochem. Sci. 23*, 257−260.
16. Tucker, J., Sczakiel, G., Feurstein, J., John, J., Goody, R. S., and Wittinghofer, A. (1986) *EMBO J. 5*, 1351−1358.
17. Gibbs, J. B., Sigal, I. S., Poe, M., and Scolnick, E. M. (1984) *Proc. Natl. Acad. Sci. U.S.A. 81*, 5704−5708.
18. Deng, H., Wang, J., Ray, W. J., and Callender, R. (1998) *J. Phys. Chem. B 102*, 3617−3623.
19. Wang, J. H., Xiao, D. G., Deng, H., and Callender, R. (1998) *Biospectroscopy 4*, 219−228.

20. Manor, D., Weng, G., Deng, H., Cosloy, S., Chen, C. X., Balogh-Nair, V., Delaria, K., Jurnak, F., and Callender, R. H. (1991) *Biochemistry 30*, 10914−10920.
21. Wang, J. H., Xiao, D. G., Deng, H., Webb, M. R., and Callender, R. (1998) *Biochemistry 37*, 11106−11116.
22. Deng, H., Wang, J., Callender, R. H., Grammer, J. C., and Yount, R. G. (1998) *Biochemistry 37*, 10972−10979.
23. Brown, I. D., and Shannon, R. D. (1973) *Acta Crystallogr. A29*, 1957−1959.
24. Brown, I. D. (1992) *Act. Crystallogr. B48*, 553−572.
25. Brown, I. D., and Wu, K. K. (1976) *Acta Crystallogr. B32*, 1957−1959.
26. Ray, J. W. J., Burgner, I. J. W., Deng, H., and Callender, R. (1993) *Biochemistry 32*, 12977−12983.
27. John, J., Rensland, H., Schlichting, I., Vetter, I., Borasio, G. D., Goody, R. S., and Wittinghofer, A. (1993) *J. Biol. Chem. 268*, 923−929.
28. Tong, L., de Vos, A. M., Milburn, M. V., and Kim, S. H. (1991) *J. Mol. Biol. 217*, 503−516.
29. Herschlag, D., and Jencks, W. (1986) *J. Am. Chem. Soc. 108*, 7938−7946.
30. DiSabato, G., and Jencks, W. (1986) *J. Am. Chem. Soc. 108*, 7938−7946.
31. Admiraal, S. J., and Herschlag, D. (1995) *Chem. Biol. 2*, 729−739.
32. Maegley, K. A., Admiraal, S. J., and Herschlag, D. (1996) *Proc. Natl. Acad. Sci. U.S.A. 93*, 8160−8166.

BI0021131